acetic acid and lyophilized. The amino acid composition was analyzed at the University of California, Davis, and shown to be within 10% of theoretical values. High-performance liquid chromatography analysis indicated purity in the range of 60 to 80%. Additional peptides (PV-22/23, PV-23/24, VTCG, and VGVRVR) were synthesized by American Peptide Co. (Santa Clara, CA) and were >95% pure. Peptides were stored at −20°C under argon to protect against oxidation, and solutions were prepared immediately before use. The free sulfhydryl group content of solutions of cysteine-containing peptides was routinely tested with Ellman's reagent (Pierce Chemical Co., Rockford, IL) by spectrophotometric assay. Except for PV-22, which showed a tendency to form dimers in solution, the cysteine residues of peptides PV-21, PV-23, PV-22/23, and VTCG remained predominantly (>80%) in reduced form.

11. Plastic microtiter plates (eight-well strips, Costar) were coated with 100 μl of peptides or, as a control, bovine serum albumin (BSA), diluted to 10 μg/ml in 0.1 M carbonate buffer (pH 9.6) and incubated at 4°C overnight. Peptide solutions (1 mg/ml in distilled water) were prepared just before their use in assays. Nonspecific sites were blocked with 1% BSA–phosphate-buffered saline (PBS) for 3 hours at room temperature. Cells were labeled with ^{51}Cr (100 μCi per 10^7 cells/ml) in RPMI 1640 containing 5% fetal bovine serum (FBS) by incubation at 37°C for 1.5 hours. After three washes, cells were resuspended in RPMI 1640 containing 1% BSA (10^6 cells/ml) and 100-μl aliquots were added in triplicate to the microtiter plates. After a 1-hour incubation at 37°C, a Transtar device (Costar) was used to remove the nonadherent cells, and then the places were washed twice with PBS. The individual wells were separated and counted in a gamma counter. Cell lines were obtained from the American Type Culture Association, except for the small-cell lung tumor lines H82 and H446, which were obtained from A. Doyle. All lines were maintained in RPMI 1640 medium supplemented with 10% FBS and subcultivated twice weekly. Experiments were conducted with cells in log phase growth and were repeated at least three times.
12. K. A. Rich *et al.*, unpublished observations.
13. P. J. Barr *et al.*, *J. Exp. Med.* **165**, 1160 (1987).
14. The single-letter abbreviations for the amino acid residues are A, Ala; C, Cys; D, Asp; E, Glu; F, Phe; G, Gly; H, His; I, Ile; K, Lys; L, Leu; M, Met; N, Asn; P, Pro; Q, Gln; R, Arg; S, Ser; T, Thr; V, Val; W, Trp; and Y, Tyr.
15. Peptides or CS proteins were labeled in aqueous solution at pH 8.6 with FITC bound to cellulose powder [H. Rinderknecht, *Nature* **193**, 167 (1962)] and then desalted by G-10 or G-25 chromatography. CEM cells (2×10^5 per tube) were incubated with FITC-labeled proteins (50 μg/ml) for 30 min at 37°C, washed, and analyzed with a FACStar Plus flow cytometer (Becton Dickinson).
16. E. Ruoslahti and M. D. Pierschbacher, *Cell* **44**, 517 (1986).
17. J. Graf *et al.*, *Biochemistry* **26**, 6896 (1987).
18. R. O. Hynes, *Cell* **48**, 549 (1987).
19. D. E. Staunton, S. D. Marlin, C. Stratowa, M. L. Dustin, T. A. Springer, *ibid.* **52**, 925 (1988).
20. M. P. Bevilacqua, S. Stengelin, M. A. Gimbrone, Jr., B. Seed, *Science* **243**, 1160 (1989).
21. M. H. Siegelman, M. Van de Rijn, I. L. Weissman, *ibid.*, p. 1165.
22. I. Stamenkovic, M. Amiot, J. M. Pesando, B. Seed, *Cell* **56**, 1057 (1989); L. A. Goldstein *et al.*, *ibid.*, p. 1063.
23. M. E. Hemler *et al.*, *J. Biol. Chem.* **262**, 11478 (1987); M. E. Hemler *et al.*, *Immunol. Today* **9**, 109 (1988).
24. M. D. Pierschbacher and E. Ruoslahti, *Nature* **309**, 30 (1984); S. K. Akiyama and K. M. Yamada, *J. Biol. Chem.* **260**, 10402 (1985); M. A. Boudon and E. Ruoslahti, *J. Cell Biol.* **108**, 1149 (1989); H.-G. Klingemann and S. Dedhar, *Blood* **74**, 1348 (1989).
25. J. M. Thornton, *J. Mol. Biol.* **151**, 261 (1981).
26. V. Nussenzweig and R. S. Nussenzweig, *Cell* **42**, 401 (1985).
27. D. C. Kaslow *et al.*, *Nature* **333**, 74 (1988).
28. D. E. Arnot, J. W. Barnwell, M. J. Stewart, *Proc. Natl. Acad. Sci. U.S.A.* **85**, 8102 (1988).
29. We thank K. Callahan for expert technical assistance, C.-M. Chuong for helpful discussions, and I. Bathurst of Chiron Corporation (Emeryville, CA) for kindly providing the CS protein preparations. Supported by a contract (DPE-0453-C-00-6060-00) from the U.S. Agency for International Development.

15 March 1990; accepted 9 July 1990

Molecular Analysis of Acute Promyelocytic Leukemia Breakpoint Cluster Region on Chromosome 17

JULIAN BORROW, AUDREY D. GODDARD, DENISE SHEER, ELLEN SOLOMON

Acute promyelocytic leukemia (APL; FAB M3) is characterized by a predominance of malignant promyelocytes that carry a reciprocal translocation between the long arms of chromosomes 15 and 17, t(15;17)(q22;q11.2–q12). This translocation has become diagnostic for APL, as it is present in almost 100 percent of cases. A Not I linking clone was used to detect this translocation initially on pulsed-field gel electrophoresis and subsequently with conventional Southern (DNA) analysis. The breakpoints in ten APL cases examined were shown to cluster in a 12-kb region of chromosome 17, containing two CpG-rich islands. The region is the first intron of the retinoic acid receptor α gene (*RARA*).

ACUTE PROMYELOCYTIC LEUKEMIA (APL) is associated with hypofibrinogenaemia and severe early hemorrhage attributable to the abundance of neoplastic promyelocytes (*1*). Treatment of this attendant coagulopathy necessitates early and accurate diagnosis of the disease. The presence of a consistent chromosomal translocation t(15;17) (*2*) (Fig. 1) in the promyelocytes of the majority of APL patients suggests the location of oncogenic sequences that are rearranged during the leukemogenic process and whose identification would help elucidate the mechanisms of transformation. In other leukemias in which nonrandom translocations have been observed, such as Burkitt's lymphoma (*3*) and chronic myelogenous leukemia (*4*), breakpoint analysis was only possible because there was previous knowledge of the genes that mapped to the breakpoint region. In APL the candidate genes *MPO*, *thra*-1, and c-*erb*B2 have not been reported to be molecularly rearranged (*5*), requiring a broader physical approach to the cloning of the breakpoint.

Translocation breakpoints can be visualized as alterations in rare-cutter fragment sizes on pulsed-field gel electrophoresis (PFGE) (*6*). The use of linking clones (*7*), which span rare-cutter sites, simplifies the detection of these rearrangements (*8*) and helps in the construction of long-range physical maps. In addition, these clones mark the position of a subset of the genes in a defined region (*9*). We constructed a Not I linking library from an interspecies hybrid TRID62 (*10*), which contains 17q as its only human material, to identify Not I sites that flank the APL breakpoint. This library and the sublocalization of 112 human clones over a chromosome 17 mapping panel will be described elsewhere.

The linking clones LCN4A3 (D17S273) and LCN2C11 (D17S163) that were found to flank the APL breakpoint (Fig. 1) were used as probes on PFGE. Unique probes were isolated from both sides of the Not I site and hybridized to somatic cell hybrids containing either the 15q+ or 17q− APL derivative chromosome and to normal controls. Subclone LCN4A3/A (Figs. 2B and 3), which mapped distal to the breakpoint, detected abnormal PFGE band sizes. In Not I digests, the normal fragment of 170 kb was rearranged to 310 kb by the translocation (Fig. 2A). This 310-kb band was the only band detected in two independent 15q+ interspecies hybrids [PJT2A1 (*11*) and PLTI1S (*12*)] constructed from different patients with APL, whereas both the normal and translocated bands were present in bone marrow samples from three other patients (APL 512, APL 511, and APL 510). A sample from patient APL 510 during remission (APL 510-R) did not show the 310-kb band, demonstrating a strong correlation between the genomic rearrangements and the neoplastic state. Single cases of both FAB M1 and FAB M2 leukemias (undifferentiated and myeloblastic acute nonlymphocytic leukemia, respectively) also appeared structurally normal in this region as expected, since the t(15;17) is not associated with these diseases. An extension of the PFGE

J. Borrow, A. D. Goddard, E. Solomon, Somatic Cell Genetics Laboratory, Imperial Cancer Research Fund, London WC2A 3PX, United Kingdom.
D. Sheer, Human Cytogenetics Laboratory, Imperial Cancer Research Fund, London WC2A 3PX, United Kingdom.

analysis revealed further band shifts from 530 kb to 790 kb and from 220 kb to 800 kb for Cla I and Mlu I, respectively (*13*).

The second cluster of rare-cutter sites between LCN4A3/A and the breakpoints (Figs. 2B and 3) prevented detection of rearranged bands with Bss HII, Eag I, Sac II, or Nar I with this probe, although the two islands are only 3 kb apart. Subclones from the distal (LCN4A3/B) and proximal (LCN4A3/C) sides of these two clusters (Fig. 3) revealed additional CpG-rich islands ~23 kb in both directions (Figs. 2B, 3). Cosmid clones were obtained that encompassed all four islands and contained the entire APL breakpoint region.

Hybridization of conventional gel electrophoresis blots with appropriate single-copy probes from this region revealed alterations in all 11 APL samples analyzed, 7 of which are shown in Fig. 3. DNA from a human-mouse hybrid, PCTBA1.8 (*14*), containing chromosome 17 as its only karyotypically visible human material, showed human bands of 10 kb and 5.4 kb and one mouse band (Fig. 4A, lane 1) when digested with Eco RI and probed with LCN4A3/A. The same probe detects novel Eco RI fragments and not the normal fragments in the somatic cell hybrids PJT2A1, PLTI1S, and GBT8 (*15*), which contain only 15q+ derivative chromosomes and no normal chromosome 17 (Fig. 4A, lanes 3, 4, and 5). The hybrid GBT8 was derived from patient APL 511, whose blood is shown in Fig. 4A, lane 6. The hybrid and blood DNA share the same rearranged band, whereas the blood has additional 10- and 5.4-kb bands because of the presence of the normal chromosome 17. Novel Eco RI fragments were also observed in an additional four blood samples (Fig. 4A, lanes 7, 8, 13, and 14). In these samples LCN4A3/A detected both the altered 15q+ derivative bands and the normal Eco RI bands of 10 kb and 5.4 kb. A further two patients (514 and 524) also showed rearrangements in this region (*16*) (Fig. 3).

Subclone LCN4A3/C was absent from the three 15q+ hybrids, indicating that it lies on the 17q− translocation product. This probe was used to detect the reciprocal 17q− derivatives in four of the APL patients as aberrant Eco RI fragments (Fig. 4B, lanes 6, 7, 8, and 14). Thus, the reciprocal breakpoints in these four tumors lie within the 10 kb defined by the boundaries of probes LCN4A3/A and LCN4A3/C and no substantial loss of genomic material occurred on translocation. The 15q+ breakpoints in hybrids PJT2A1 and PLTI1S also occur in this region (Figs. 3 and 4A). Bone marrow (BM) and blood lymphocyte (BL) remission samples from patient APL 510 [APL 510-R (BM) and APL 510-R (BL)] (Fig. 4A, lanes 9 and 10) had lost the altered bands. FAB M1 and FAB M2 (Fig. 4A, lanes 11 and 12) were also unrearranged in this region, confirming our PFGE results.

For patient APL 2726, a Hind III digest was required to reveal a band shift with probe LCN4A3/A, whereas the breakpoint of the 17q− hybrid P12.3B6 (*17*) was located about 20 kb proximal to the other breakpoints (*18*) (Fig. 3). Thus, 10 of 11 translocations (both 15q+ and 17q−) fell within a 12-kb region. Only the breakpoint in the 17q− contained in the hybrid P12.3B6 was located outside this region. Analysis of the corresponding 15q+ chromosome would determine if the break in P12.3B6 is reciprocal or associated with a deletion.

LCN4A3/B was used to screen an HL60 cDNA library. The five positive clones obtained were sequenced (*19*) and mapped with respect to one another and the corresponding genomic DNA (Fig. 3B). Sequence comparison with the EMBL database revealed the cDNA to be that of *RARA* (*20*). Since *RARA* had been mapped to 17q21.1 (*21*), distal to the APL breakpoint region (17q11.2-12), we wanted to demonstrate that the gene located at the APL

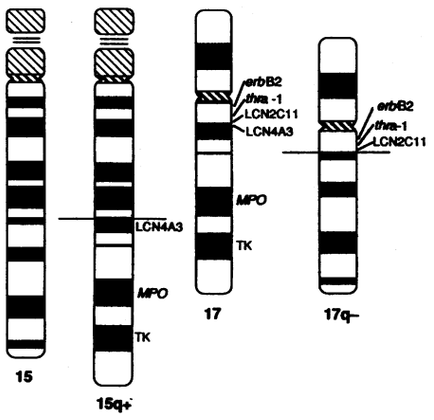

Fig. 1. Schematic representation of the APL translocation showing the derivative 15q+ and 17q− chromosomes. The positions of the Not I linking clones that flank the APL breakpoint (LCN4A3 and LCN2C11) are shown, together with the approximate positions of former candidate genes, *erb*B2, *thra*-1, and myeloperoxidase (*MPO*). TK, thymidine kinase.

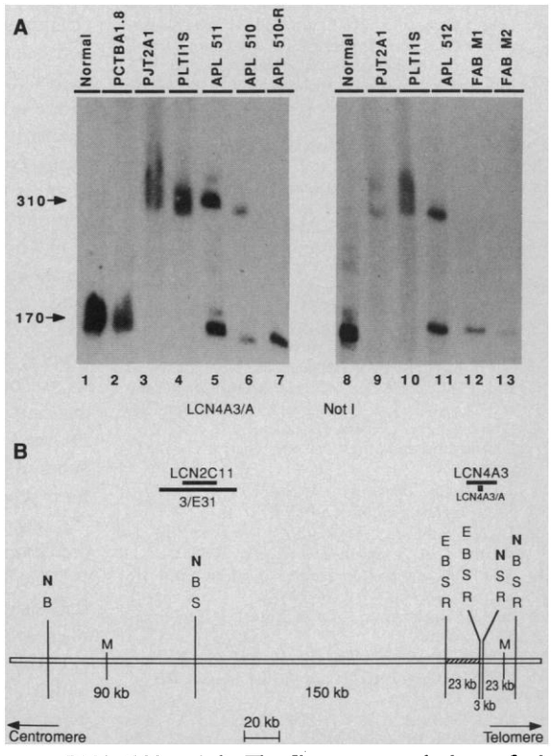

Fig. 2. (**A**) Pulsed-field gel analysis with probe LCN4A3. A 3-kb Bam HI–Not I fragment from LCN4A3 (LCN4A3/A, Fig. 3) was hybridized to Not I digests of the following DNA samples: Normal, normal lymphoblastoid line; PCTBA1.8, chromosome 17–only hybrid; PJT2A1 and PLTI1S, 15q+ hybrids; APL 511, APL 510, and APL 512, blood samples from APL patients; APL 510-R, bone marrow sample from patient APL 510 during remission; FAB M1 and FAB M2, blood samples from undifferentiated and myeloblastic acute nonlymphocytic leukemia, respectively. DNA was prepared from cells resuspended in 0.6% low melting point agarose at a concentration of 1×10^6 cells per block as described (*27*) and digested with 40 units of Not I per block. Pulsed-field gels were run on the LKB 2015 Pulsaphor system with a hexagonal electrode configuration. The 1% agarose gel was run in 0.25× tris-borate-EDTA buffer at 170 volts with a 25-s pulse time for 40 hours. After transfer to Hybond N^+, hybridization with oligolabeled probes (*28*) was performed in 5× SSC, 0.1% SDS, 5× Denhardt's, 50% formamide, and salmon sperm DNA (100 μg/ml). The filters were washed to a final stringency of 0.1× SSC and 0.1% SDS at 65°C. Probes were competed with sheared human DNA where necessary (*29*). (**B**) Pulsed-field map of the APL region on chromosome 17 with the cross-hatched area representing the region containing the five 15q+ breakpoints in PJT2A1, PLTI1S, APL 510, APL 511, and APL 512. The exact points of breakage within this region appeared to be the same within the resolution of the gels. Rare-cutting enzyme sites: N, Not I; E, Eag I; B, Bss HII; S, Sac II; M, Mlu I; and R, Nar I. The position of the linking clone LCN4A3, the cosmid 3/E31, and its corresponding linking clone LCN2C11 are indicated by solid bars above the map. The cosmid 3/E31 was isolated from a KLT8 cosmid library, mapped immediately proximal to APL (*30*), and used to isolate LCN2C11 from the linking library.

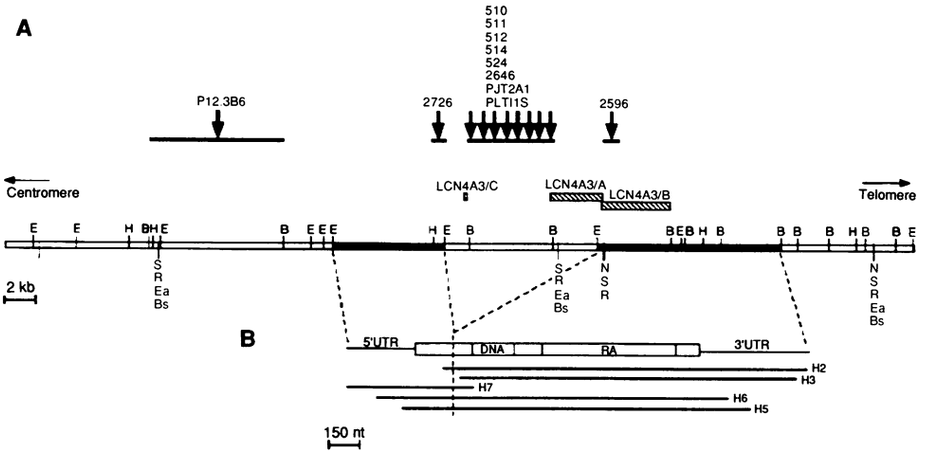

Fig. 3. (**A**) restriction map of the APL breakpoint region. The location of the breakpoints in nine APL samples are indicated with arrows above the smallest restriction fragment to which the breaks have been positioned. B, Bam HI; E, Eco RI; H, Hind III; N, Not I; Ea, Eag I; Bs, Bss HII; S, Sac II; and R, Nar I. Clusters of rare-cutting enzyme sites are indicated below the map. Fragments used in analysis of the region are indicated by rectangles above the map. Stippled boxes, restriction fragments containing exons of *RARA*. (**B**) *RARA* cDNA. Open box, coding sequences. DNA binding and retinoic acid binding domains are indicated. The 5′ and 3′ untranslated sequences (UTRs) are shown as solid lines. The cDNAs isolated from a PMA-stimulated HeLa cDNA library are indicated below the cDNA by solid bars. Dashed lines show location of the first intron and the approximate location of exons in the genomic DNA.

breakpoint was indeed *RARA* rather than a similar member of the nuclear receptor superfamily. The cDNA was hybridized to both total human and cosmid DNA from the region to show that our breakpoint region restriction map and the bands detected by DNA hybridization matched the published band pattern detected with a *RARA* cDNA (*20*). By mapping the positions of the 5′ ends of two of our cDNAs (H2 and H3) onto genomic DNA we were able to demonstrate that the cDNAs hybridized to sequences on either side of the translocation breakpoints, but not in the 12 kb breakpoint region (Fig. 3). From the published amino acid and cDNA sequences we deduced that this discontinuity between the genomic and cDNA clones represented the first intron of *RARA* (*20*). All of the 15q+ APL breakpoints lie within this region (Fig. 3A).

Analysis of nonrandom translocations associated with other hematopoietic malignancies has led to identification of both previously known and novel oncogenes (*22*). For example, translocation of c-*myc* into the immunoglobulin loci results in its deregulation in Burkitt's lymphoma. The novel fusion proteins expressed by *bcr/abl* and *E2A/prl*, produced as the result of translocations in chronic myelogenous leukemia and pre-B leukemia, respectively, have been implicated in malignancy (*22*). In the T-ALL cell line RPMI 8402, multiple gene are deregulated by the translocation (*22*).

Since *RARA* is interrupted in an intron it is most likely that the product of the translocation is a fusion protein. As at least one 17q−breakpoint is outside this region (see P12.3B6, Fig. 3A), this suggests that the 15q+ derivative is the crucial product of the translocation. The fusion protein encoded by the 15q+ derivative would retain the DNA- and ligand-binding domains of *RARA*. The transcription-activating function of the 5′ end of the *RARA* (*23*) would be replaced with a novel NH_2-terminus hence potentially changing the profile of genes activated. The involvement of *RARA* at the APL breakpoint may explain why the use of retinoic acid as a therapeutic differentiation agent in the treatment of the acute myeloid leukemias is limited to APL (*24*).

To obtain the sequences on chromosome 15 that are juxtaposed next to *RARA*, we prepared a genomic library from the 15q+ hybrid PLTI1S and screened with LCN4A3/A (*25*). A breakpoint clone, fqp12, was obtained that contained sequences on both chromosomes as judged by its hybridization to somatic cell hybrids PCTBA1.8 (17 only) and HORL-I (*26*), which contains only human chromosome 15 and a fragment of human chromosome 11. Preliminary data with a subclone from fqp12 confirmed the clustering of breakpoints on chromosome 15 in the three patients analyzed. Characterization of these

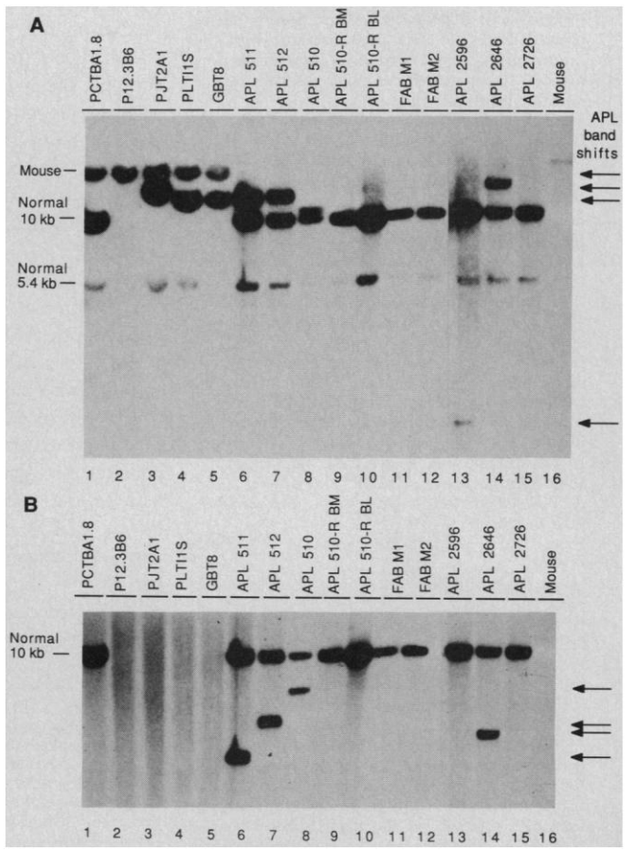

Fig. 4. Detection of the APL breakpoints on Southern blot analysis. DNA from blood samples from APL patients and mouse-human hybrids containing APL-derivative chromosomes, when digested with Eco RI, demonstrate rearranged junction fragments. DNA samples APL 511, APL 512, APL 510, APL 2596, APL 2646, and APL 2726 represent six different APL patients; PJT2A1, PLTI1S, and GBT8, three APL 15q+ mouse-human hybrids (GBT8 is derived from patient APL 511); P12.3B6, an APL 17q− mouse-human hybrid; PCTBA1.8, chromosome 17–only hybrid; APL 510-R (BM) and APL 510-R (BL), bone marrow and blood lymphocyte remission samples from patient APL 510; and FAB M1 and FAB M2 are cases of undifferentiated and myeloblastic acute nonlymphocytic leukemia, respectively. (**A**) Subclone LCN4A3/A detects the 15q+ rearrangements in seven of eight samples on Eco RI digests. The rearranged band in APL 2596 is fainter than the other novel bands as it is derived from the 5.4-kb normal band and not the 10-kb normal band. (**B**) After stripping the filter, subclone LCN4A3/C, a unique 200-bp Bam HI–Pst I fragment (Fig. 3), was used to detect the 17q− derivative chromosome on Eco RI digests in four APL patients.

sequences, together with *RARA* should allow a full molecular description of APL.

Note added in proof. Lemmons *et al.* have also reported the cloning of the APL breakpoint region (*31*).

REFERENCES AND NOTES

1. L. K. Hillestad, *Acta Med. Scand.* **159**, 189 (1957).
2. R. A. Larson *et al.*, *Am. J. Med.* **76**, 827 (1984); D. Sheer *et al.*, *Br. J. Cancer* **52**, 55 (1985).
3. R. Dalla-Favera *et al.*, *Proc. Natl. Acad. Sci. U.S.A.* **79**, 7824 (1982).
4. A. De Klein *et al.*, *Nature* **300**, 765 (1982).
5. P. van Tuinen *et al.*, *Oncogene* **1**, 319 (1987); C. W. Miller *et al.*, *Science* **244**, 823 (1989); E. Donti *et al.*, *ibid.*, p. 824; S. C. Weil *et al.*, *ibid.*, p. 825.
6. C. L. Smith and C. R. Cantor, *Methods Enzymol.* **155**, 449 (1987).
7. A. Poustka and H. Lehrach, *Trends Genet.* **2**, 174 (1986).
8. A. M. Frischauf, *Technique* **1**, 3 (1989).
9. A. P. Bird, *Trends Genet.* **3**, 342 (1987).
10. A. Tunnacliffe *et al.*, *EMBO J.* **2**, 1577 (1983).
11. D. Sheer *et al.*, *Proc. Natl. Acad. Sci. U.S.A.* **80**, 5007 (1983).
12. G. Moore *et al.*, *Genomics* **4**, 152 (1989).
13. J. Borrow and A. Goddard, unpublished.
14. Y. Bai *et al.*, *Ann. Hum. Genet.* **46**, 337 (1982).
15. GBT8 is a mouse-human somatic cell hybrid constructed from patient APL 511 by P. Gorman and D. Sheer. It contains the APL 15q+ derivative chromosome but no normal chromosome 15 or 17.
16. J. Borrow and A. Goddard, unpublished.
17. P. van Tuinen *et al.*, *Genomics* **1**, 374 (1987).
18. A. Goddard and J. Borrow, unpublished.
19. Colonies (5×10^5) from a PMA-stimulated HL60 cDNA library (a gift from D. Simmons, Oxford) constructed in the plasmid vector CDM8 were screened with LCN4A3/B and five positive clones purified. Sequence data were obtained with the Sequenase Kit from United States Biochemical Corporation and assembled and analyzed with programs from IntelliGenetics Inc.
20. M. Petkovich *et al.*, *Nature* **330**, 444 (1987); V. Giguere *et al.*, *ibid.*, p. 624.
21. M. G. Mattei *et al.*, *Hum. Genet.* **80**, 186 (1988).
22. C. M. Croce, *Cell* **49**, 155 (1987); Y. Ben-Neriah *et al.*, *Science* **233**, 212 (1986); J. Nourse *et al.*, *Cell* **60**, 535 (1990); E. A. McGuire *et al.*, *Mol. Cell. Biol.* **9**, 2124 (1989).
23. S. Green and P. Chambon, *Trends Genet.* **4**, 309 (1988).
24. T. R. Breitman, S. J. Collins, B. R. Keene, *Blood* **57**, 1000 (1981); Z. Y. Wang *et al.*, *Nouv. Rev. Fr. Hematol.* **32**, 25 (1990).
25. A genomic library was prepared from the 15q+ mouse-human hybrid PLTI1S in EMBL3*cos*. LCN4A3/A was used to screen 1.5×10^6 recombinant phage and breakpoint clone fqp12 was isolated.
26. N. Heisterkamp *et al.*, *Nature* **299**, 747 (1982).
27. B. G. Herrmann *et al.*, *Cell* **48**, 813 (1987).
28. A. P. Feinberg and B. Vogelstein, *Anal. Biochem.* **132**, 6 (1983).
29. P. G. Sealey *et al.*, *Nucleic Acids Res.* **13**, 1905 (1985).
30. M. K. Yagle *et al.*, *Proc. Natl. Acad. Sci. U.S.A.*, in press.
31. R. S. Lemmons *et al.*, *Genes Chrom. Cancer* **2**, 79 (1990).

32. We are grateful to A.-M. Frischauf and H. Himmelbauer for advice on the construction of the linking library and use of a genomic cosmid library, and to D. H. Ledbetter for the cell line P12.3B6. We thank A. Lister, A. Rohatiner, and B. Gibbons at St. Bartholomew's Hospital, London, J. Chessels and F. Katz at Great Ormond Street, London, and I. Dube at the University of Toronto for collecting samples from APL patients. We also thank S. Rider and P. Hedge for pulsed-field blocks of DNA and for helpful discussions on APL.

25 June 1990; accepted 14 August 1990

Flip and Flop: A Cell-Specific Functional Switch in Glutamate-Operated Channels of the CNS

BERND SOMMER,* KARI KEINÄNEN,*† TODD A. VERDOORN, WILLIAM WISDEN, NAIL BURNASHEV, ANNE HERB, MARTIN KÖHLER, TAMAKI TAKAGI, BERT SAKMANN, PETER H. SEEBURG‡

In the central nervous system (CNS), the principal mediators of fast synaptic excitatory neurotransmission are L-glutamate–gated ion channels that are responsive to the glutamate agonist α-amino-3-hydroxy-5-methyl-4-isoxazole propionic acid (AMPA). In each member of a family of four abundant AMPA receptors, a small segment preceding the predicted fourth transmembrane region has been shown to exist in two versions with different amino acid sequences. These modules, designated "flip" and "flop," are encoded by adjacent exons of the receptor genes and impart different pharmacological and kinetic properties on currents evoked by L-glutamate or AMPA, but not those evoked by kainate. For each receptor, the alternatively spliced messenger RNAs show distinct expression patterns in rat brain, particularly in the CA1 and CA3 fields of the hippocampus. These results identify a switch in the molecular and functional properties of glutamate receptors operated by alternative splicing.

L-GLUTAMATE (L-GLU), THE MAJOR excitatory neurotransmitter in the mammalian CNS exerts its diverse effects through pharmacologically distinct receptors (*1*). Fast synaptic neurotransmission is thought to be mainly mediated by cationic channels intrinsic to AMPA-gated receptors. Kainate has been suggested to gate a second subtype of glutamate receptor mediating fast neurotransmission. Synaptic transmission mediated by a third receptor subtype, the *N*-methyl-D-aspartate (NMDA) receptor, is characterized by a slow rise time, voltage-dependent block by Mg^{2+}, and Ca^{2+} permeability; these channels induce various forms of activity-dependent synaptic plasticity such as long-term potentiation (LTP) (*2*). However, maintenance of the LTP-associated synaptic enhancement can require, at least in part, a change in postsynaptic AMPA receptors (for example, in the CA1 area of the hippocampus) (*2, 3*).

We have analyzed by molecular cloning the family of AMPA receptors in the CNS (*4*). These receptors bind AMPA, and their channels are gated by AMPA, L-Glu, and kainate, indicating a blurred distinction between AMPA and kainate receptors that varies depending if they are classified by gating or by ligand binding. The properties of these receptors are consistent with electrophysiological data from hippocampal neurons that suggest that AMPA and kainate act predominantly on the same receptor (*5*). We now describe the existence and function of a second molecular version of the four AMPA receptors, generated by alternative splicing.

Molecular cloning and detailed analysis of cDNAs encoding the AMPA-selective glutamate receptors GluR-A, -B, -C, and -D (*4*) revealed that in each receptor a segment of 115 bp exists in one of two sequence versions. This segment encodes 38 amino acid residues within a conserved receptor domain preceding the predicted fourth transmembrane region (Fig. 1) and hence is probably located intracellularly (*4, 6*). The alternative versions were named "flip" and "flop," with the previously described primary structures (*4*) as the flop forms. In each of the receptors, the sequences of the two alternative segments are very similar, and most nucleotide substitutions are silent changes with respect to the protein sequence. Accordingly, the flip and flop versions of each polypeptide differ in only a few (9 to 11) amino acids, and these substitutions are often conservative. A tetrapeptide is consistently different between the two versions of the four receptors. Neither of the alternative tetrapeptides conforms to known consensus sequences.

The exchange of small homologous domains in four glutamate receptors suggested that the two receptor versions for each of the four family members arose from alternative splicing. Such a mechanism was further implied by high resolution mapping and DNA sequence analysis of the murine gene for the GluR-B receptor. In this gene, the flip and flop sequences are on adjacent exons, separated from each other by an intron of approximately 900 bp and from their neigh-

B. Sommer, K. Keinänen, W. Wisden, A. Herb, M. Köhler, T. Takagi, P. H. Seeburg, Laboratory of Molecular Neuroendocrinology, Center for Molecular Biology, University of Heidelberg, 6900 Heidelberg, F.R.G.
T. A. Verdoorn, N. Burnashev, B. Sakmann, Abteilung Zellphysiologie, Max-Planck-Institut für Medizinische Forschung, 6900 Heidelberg, F.R.G.

*The first two authors contributed equally to this report.
†Present address: Biotechnical Laboratory, Technical Research Center, Espoo, Finland.
‡To whom correspondence should be addressed.